

High Temperature Oxidation Behavior of Co-Cr-Y₂O₃ Modified Aluminide Coatings on Ni-based Superalloy by Pack Cementation Process

Cao Jiangdong¹, Gong Shaojun¹, Zhong Chonggui², Yao Yanbin³

¹ Jiangsu Shipping College, Nantong 226010, China; ² Nantong University, Nantong 226001, China; ³ Research and Development Department, Shenzhen PIM Technology CO. LTD, Shenzhen 518001, China

Abstract: The microstructure and high temperature oxidation behavior of Co-Cr-Y₂O₃ modified pack aluminide coatings on Ni-based superalloy GH586 were investigated. The results show that the specific Co-Cr-Y₂O₃ modified aluminide coating has a mass gain of only 0.36 mg/cm² after oxidation at 1000 °C for 100 h, which is much less than that of the substrate at 1000 °C. From X-ray diffraction, the phase of the coatings is mainly AlNi, and after oxidation at 1000 °C for 100 h the denser oxidation scale is composed of Al₂O₃, Cr₂O₃, and CoCr₂O₄. Surface and cross sectional morphologies were characterized by scanning electron microscope (SEM). The coating exhibits a better resistance to high temperature oxidation, compared to the oxidation film of GH586 without coating. Moreover, the growing Cr (W) rich phase is gradually gathered at the grain boundaries during the oxidation, and it is beneficial to providing more Cr element for the dense oxidation film, which is mainly attributed to the excellent high temperature oxidation resistance.

Key words: superalloy; oxidation behavior; surface modification; coating

Since Ni-based superalloys have excellent mechanical strength and high-temperature oxidation at 800~900 °C, they have been extensively applied in the gas-turbine industry^[1]. However, as superalloys are easier to oxidize and corrode at operating temperatures, layer coatings are needed to protect alloys from high oxidation and corrosion^[2]. MCrAlY coatings are widely used as an overlayer at the high temperature to protect alloy by forming a dense and continuous alumina scale to prevent the inward diffusion of oxygen^[3-5]. There are various preparative techniques for depositing MCrAlY coatings, particularly, the Electron-beam physical deposition (EB-PVD), magnetron sputtering and atmospheric plasma-sprayed (APS)^[6,7]. However, a few drawbacks still exist in the coatings prepared by these methods. So-called line-of-sight effect^[8], coarse microstructures and non-uniform coating thickness can influence the service life of the coating. Stresses and vanes are also introduced which would accelerate

the coating failure under thermal cycling^[9-12]. In addition, the high cost of these methods deeply restricts the development of these techniques. Nowadays, pack cementation process is low in cost and can produce a uniform and smooth diffusion coating on different complex shapes, so it is frequently used in the industrial areas^[13,14]. In recent years, the benefit addition of Pt, Y, Ce, Co, Hf, Si modified aluminide coatings have been widely studied. Previously, Gong et al^[14, 15] have reported that Cr-modified aluminide coatings have good oxidation resistance and hot corrosion resistance. Zhou et al^[16-19] have studied the Co, Y, Ce and Y-Ce co-modified aluminide coatings, and found that the element addition can improve hot corrosion resistance. However, the microstructure and the oxidation resistance of the Co-Cr-Y₂O₃ modified aluminide coating have been seldom studied so far.

In this study, Cr-Co-Y₂O₃ modified aluminide coating on nickel based superalloys was prepared by pack cementation

Received date: March 31, 2018

Foundation item: Natural Science Foundation of Jiangsu Province (16KJB430035); Qing Lan Project of Jiangsu Province

Corresponding author: Cao Jiangdong, Ph. D., Associate Professor, Mechanical and Electrical Department, Jiangsu Shipping College, Nantong 226010, P. R. China, Tel: 0086-513-85960874, E-mail: caojd@ntsc.edu.cn

Copyright © 2018, Northwest Institute for Nonferrous Metal Research. Published by Elsevier BV. All rights reserved.

process. The microstructure, composition and oxidation resistance of the coating were evaluated by a comparison with the substrate. High temperature oxidation behavior of the coatings was analyzed, which would help to prepare a thermal barrier coating on the basis of these coatings.

1 Experiment

GH586 has been chosen to prepare Cr-Co-Y₂O₃ modified aluminide coatings. The nominal composition of the alloy is presented in Table 1. The samples were ground with 1000# SiC paper, and then degreased with acetone in the ultrasonic cleaner before being placed in pack powders. The pack powder mixtures were prepared using powders of Al₂O₃, Co, Al, Cr, Y₂O₃ and NH₄Cl; the average particle size of all the powder used was less than 74 μm. The composition of all pack powder mixtures is listed in Table 2. The substrate was buried by a well-mixed pack powder in an alumina crucible, which was covered by an alumina lid sealed with fire clay. After that, the pack was loaded into a tube furnace under argon protection. The temperature of the furnace was raised to 900 °C at a designed rate and held at this temperature for 9 h, and then cooled down to room temperature, and the samples were always protected by the argon gas throughout the process.

The isothermal oxidation tests were performed at 1000 °C for 100 h to evaluate the protective effect. Specimens were polished and then put into an alumina crucible. Then, the crucible was put into a timer-controlled resistance furnace for remaining the designed time. After oxidation for 1, 3, 5, 10, 20, 40, 60, 80 and 100 h the specimens were weighed by an electronic balance with a sensitivity of 10⁻⁴ g. For each test, mass gains of the three parallel samples were calculated and averaged.

The cross-sectional and surface morphologies of the coated specimens before and after oxidation were observed by scanning electron microscopy (SEM), and the element

concentration was analyzed by energy dispersive spectroscopy (EDS). The X-ray diffraction (XRD) with Cu Kα radiation (λ=0.154 18 nm) was employed to investigate the surface phase constitution before and after oxidation.

2 Results and Discussion

2.1 Microstructures of the coating

The specimens for these experiments were coded from coating 1# to 15#. Microstructures of the Co-Cr-Al coatings were analyzed on the basis of elemental distributions, coating thickness and the rate of isothermal oxidation at 1000 °C for 100 h. Compared with Co and Cr, the Al content has a significant effect on the layer thickness. The coating of sample 6# has a better property, so it was selected to present the results of microstructure analysis in this study.

The surface morphology and X-ray pattern of coating 6# are shown in Fig.1. It can be seen that the maximal grain size of the coating surface is about 5 μm, and the minimum grain size is up to nano-scale. According to the XRD pattern, the coating is mainly composed of Ni_{0.96}Al_{1.04}, a small number of NiAl, Al₉Co₂Ni and Al₁₃Cr₂, as seen in Fig.1b. Two different areas (bright and dark in color) can be distinguished at the coating surface. From the EDS analysis given in Table 3, it can be seen that the bright area (Ni, Cr-rich) and dark area (Al rich) correspond to Ni_{0.96}Al_{1.04} and NiAl, respectively, which are marked with arrows.

Fig.2 presents the cross-sectional SEM image and major elemental concentration distribution of the coating. It is observed that the coating has an obvious two-layer structure which contains an outer layer and an internal diffusion zone. As shown in Fig.2a, the total depth of the outer layer and the

Table 1 Nominal composition of GH586 (wt%)

| Al | Ti | Mo | Cr | W | Co | C | Ni |
|-----|-----|----|----|---|----|------|------|
| 1.6 | 3.2 | 8 | 19 | 3 | 11 | 0.06 | Bal. |

Table 2 Composition of Co-Cr-Al- Y₂O₃ powder mixtures (wt%)

| Coating | Co | Cr | Al | Y ₂ O ₃ | NH ₄ Cl | Al ₂ O ₃ | Thickness/μm |
|---------|----|----|----|-------------------------------|--------------------|--------------------------------|--------------|
| 1# | 5 | 10 | 5 | 4 | 4 | 72 | 20.0 |
| 2# | 5 | 10 | 7 | 4 | 4 | 70 | 17.1 |
| 3# | 7 | 10 | 5 | 4 | 4 | 70 | 16.8 |
| 4# | 7 | 10 | 7 | 4 | 4 | 68 | 18.5 |
| 5# | 10 | 20 | 5 | 4 | 4 | 67 | 21.2 |
| 6# | 10 | 20 | 7 | 4 | 4 | 55 | 23.5 |
| 7# | 10 | 20 | 10 | 4 | 4 | 52 | 22.0 |
| 8# | 5 | 20 | 5 | 4 | 4 | 62 | 15.7 |
| 9# | 5 | 20 | 7 | 4 | 4 | 60 | 21.3 |
| 10# | 5 | 20 | 10 | 4 | 4 | 57 | 28.5 |
| 11# | 7 | 20 | 5 | 4 | 4 | 60 | 16.3 |
| 12# | 7 | 20 | 7 | 4 | 4 | 58 | 17.0 |
| 13# | 7 | 20 | 10 | 4 | 4 | 55 | 27.4 |
| 14# | 10 | 10 | 5 | 4 | 4 | 67 | 12.7 |
| 15# | 10 | 10 | 7 | 4 | 4 | 65 | 14.9 |

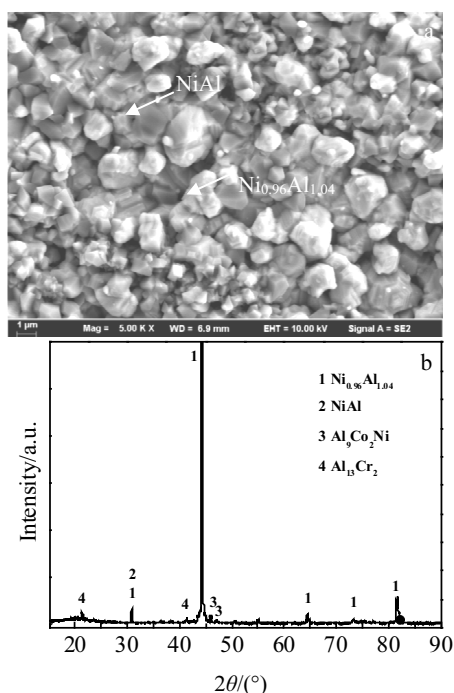


Fig.1 Surface morphology (a) and XRD pattern (b) of coating 6#

Table 3 Average chemical composition of the coating measured by EDS in Fig.1a (wt%)

| Position | Al | Cr | Co | Ni | Ti |
|-------------|-------|------|-------|-------|------|
| Bright area | 34.47 | 4.50 | 13.94 | 47.08 | 0.01 |
| Dark area | 89.68 | 1.38 | 1.71 | 7.11 | 0.12 |

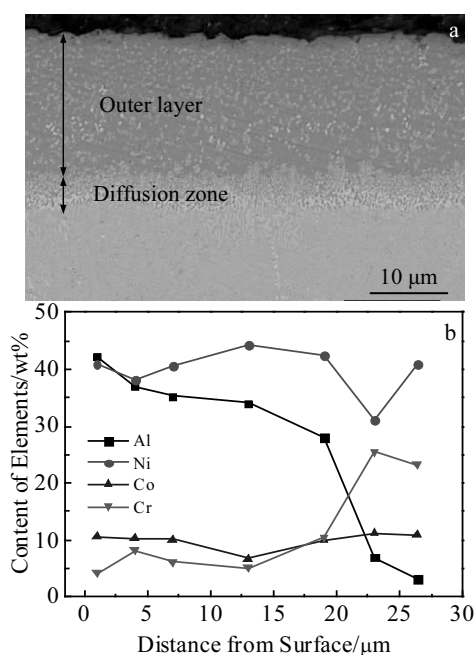


Fig.2 Cross-sectional SEM image (a) and major elemental concentration distribution (b) of the coating

diffusion zone is about 24 μm . At the high temperature, an interdiffusion zone occurs between the coating and the substrate, and the Al element diffuses into the substrate while Ni diffuses outward. It can also be found in Fig.2b that the diffusion zone exists between the coating and the substrate, which is primarily due to the outward diffusion of Ni.

2.2 Isothermal oxidation kinetics of the coating and substrate

Fig.3 presents the isothermal kinetics of the substrate and coating specimen at 1000 $^{\circ}\text{C}$ for 100 h. The oxidation kinetics shows that the substrate has poor oxidation resistance. In the initial 20 h of oxidation, both the substrate and the coated specimens have a rapid mass gain due to the formation of a layer of oxidation film on the specimen at the early oxidation. After 20~100 h, the coated specimen shows a slower rate of mass gain than the substrate, reflecting that the growth rate of the oxides is greatly decreased under the protection of a continuous and compact oxidation film. The mass gain of the substrate and the coating is 2.30 and 0.36 mg/cm^2 , respectively. It is indicated that the coating shows excellent high temperature oxidation resistance compared to the substrate at 1000 $^{\circ}\text{C}$.

2.3 Surface and cross-sectional morphologies after oxidation

The surface morphology of the substrate and coating specimens after oxidation at 1000 $^{\circ}\text{C}$ for 20 and 100 h are shown in Fig.4. In Fig.4a, a mass of big blocky-like spinels and NiO are first formed on the surface after oxidation at 1000 $^{\circ}\text{C}$ for 20 h, which is due to the lower equilibrium oxygen partial pressure of metal oxides at high temperature and the lower content of Al element in the alloy. NiO formed by the oxidation of nickel reacts with Cr_2O_3 to generate a small amount of spinels. As the oxidation continued, Cr^{3+} and Ti^{4+} diffused outward from the alloy to form finer Cr_2O_3 and TiO_2 oxides, which were found and distributed evenly at the surface. After oxidation for 100 h, TiO_2 grows up quickly and is spalled easily to form cavities. Voids and spallation are shown in Fig.4b. As shown in Fig.4c and 4d, the coating has a dense and compact surface without spallation and cracks after 20 and 100 h of oxidation testing, indicating that the coating

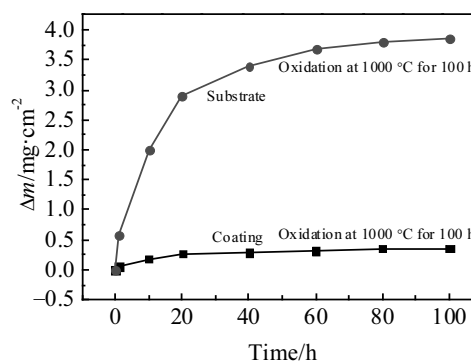


Fig.3 Isothermal kinetics of the matrix and coating specimens at 1000 $^{\circ}\text{C}$

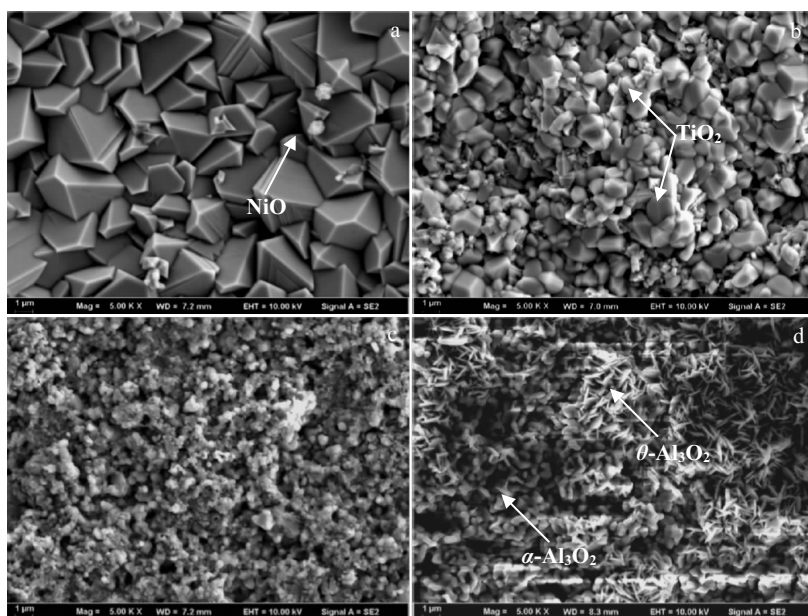


Fig.4 SEM morphologies of the substrate surfaces (a, b) and coatings (c, d) after oxidation at 1000 °C for 20 h (a, c) and 100 h (b, d)

has good high temperature oxidation resistance. When oxidation for 20 h, there are a large number of fine grains on the surface which contains a great content of Al and O elements detected by EDS. Combined with XRD analysis, these fine grains are α -Al₂O₃ with a small amount of TiO₂ distributed among them. After oxidation for 100 h, two forms of alumina formed on the surface, and combined with morphological analysis, they were identified as θ -Al₂O₃ and α -Al₂O₃.

The XRD patterns of the substrate and the coating after oxidation at 1000 °C for 20 and 100 h are shown in Fig.5. The main oxides of the substrate after oxidation for 20 h are Al₂O₃, NiO and NiCr₂O₄. When the substrate is oxidized for 100 h, Cr₂O₃ is the main phase of the oxide film because the content of Cr element in the alloy is much higher than that of Al, and a small amount of Al₂O₃ exists at the bottom of the oxide film. For the specimens with coating, Al₂O₃ is the main oxide formed after oxidation for 20 h. The phase of AlNi₃ is detected in the coating, which is transformed from the NiAl phase. As the oxidation proceeds to 100 h, spinel NiCr₂O₄ and CoCr₂O₄ appear. Co is more easily oxidized than Ni at high temperatures^[20], and it can effectively promote the formation of dense scales composed of Cr₂O₃, Cr₂O₃·CoCr₂O₄ or CoCr₂O₄. Moreover, CoO could be strongly banded to Cr₂O₃, which is beneficial to the density enhancement of oxide scale. The addition of Y can improve the oxidation and hot corrosion resistance^[21]. But in this paper, Y is not detected due to the lower content of Y. As the oxidation proceeds, the Cr and Co content decreases gradually and is insufficient to maintain the consuming, and then Ni is oxidized and forms NiCr₂O₄ by the following reaction:

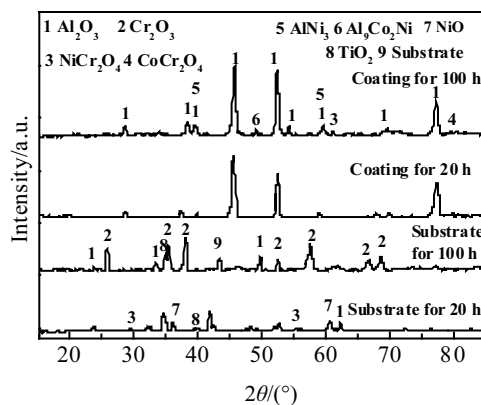


Fig.5 XRD patterns of the substrate and the coating surface after oxidation at 1000 °C for 20 and 100 h



Fig.6 shows the cross-sectional images of the substrate and coating after oxidation at 1000 °C for 20 and 100 h. Fig.6a and 6b show the substrate oxidation for 20 and 100 h at 1000 °C, respectively. A layer of loose and porous oxide scale formed on the top of the substrate. As the oxidation continued, oxygen diffused into the alloy through the oxidation scale to form the internal oxidation along the grain boundaries. Fig.6c shows the coating oxidized at 1000 °C for 20 h. At the high temperature, the Cr(W) rich phases may spread outside, diffuse in the inner or gather on the surface according to the different chemical concentration gradient. It can restrain the outward diffusion of Ti⁴⁺, delay the growth of TiO₂, keep the oxide film dense and extend the life of the coating. In Fig.6d,

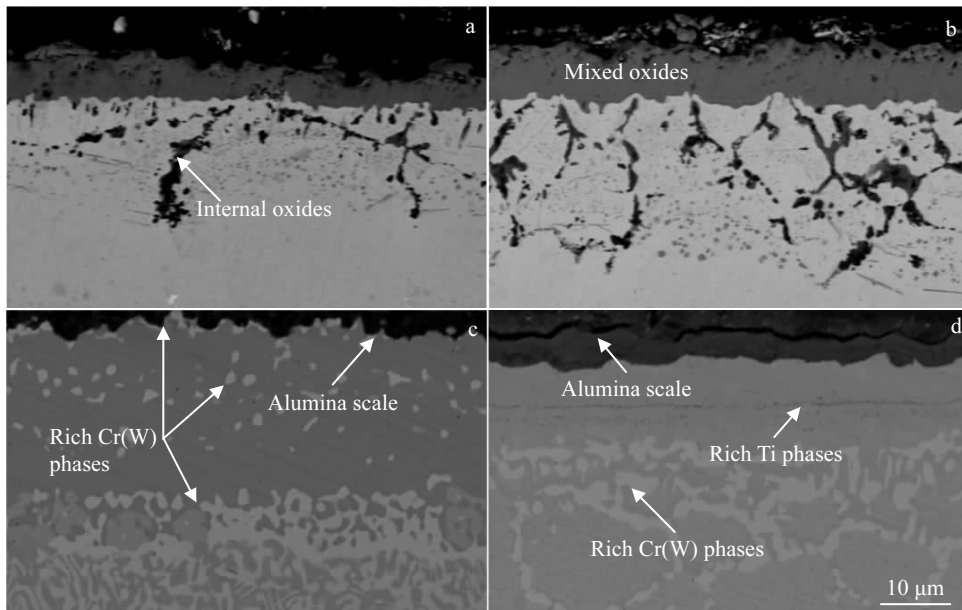


Fig.6 Cross-sectional images of the substrates (a, b) and coatings (c, d) after oxidation at 1000 °C for 20 h (a, c) and 100 h (b, d)

a continuous and compact oxidation film with a thickness of approximately 4 μm formed on the surface of the coating. From the XRD analysis in Fig.5 and the EDS, it can be concluded that the oxide on the coating surface is composed of Al_2O_3 . A discontinuous Ti-rich layer formed under the outer layer, which is similar to the report^[22]. Compared to Fig.6c, it can be found that the diffusion zone has enlarged and moved toward the outer layer. There are no voids and spallation in the aluminum oxide, illustrating that the coating has a good oxidation resistance and adhesive performance.

The EDS line scanning (element distribution) of the coating after oxidation for 20 and 100 h is shown in Fig.7. It can be seen that the oxide on the surface of the coating is mainly Al_2O_3 , and the content of Al beneath the oxidation film is gradually reduced after oxidation for 100 h due to its diffusion toward the surface of coating. According to the distribution of

Ni and Co, it is found that there is a tendency to diffuse toward the surface. And the element of Cr near the interface between the coating and the substrate is obviously gathered, which may be due to the increasing precipitation of Cr(W) with the extension of the oxidation time.

2.4 Discussion of the oxidation behavior

The rare earth oxides are more easily absorbed in the defect location of the superalloy surface than other elements. A small amount of the rare earth atoms diffuse inward along grain boundaries, resulting in a wider gap among the grains which provides many wider channels for the diffusion of other elements, as shown in Fig.8. The addition of Y_2O_3 can accelerate the formation of the Co-Cr-Al coating. Furthermore, Y_2O_3 is beneficial for improving the adhesion of oxide film.

Cr content of Ni-based superalloys is more than 15%^[23], which is beneficial for forming a continuous and dense Cr_2O_3

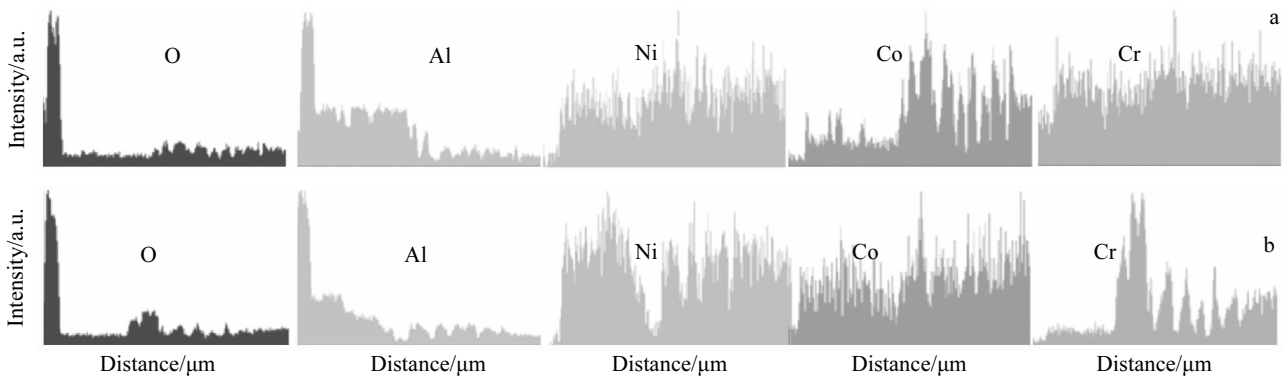


Fig.7 EDS element distributions of coatings after oxidation for 20 h (a) and 100 h (b)

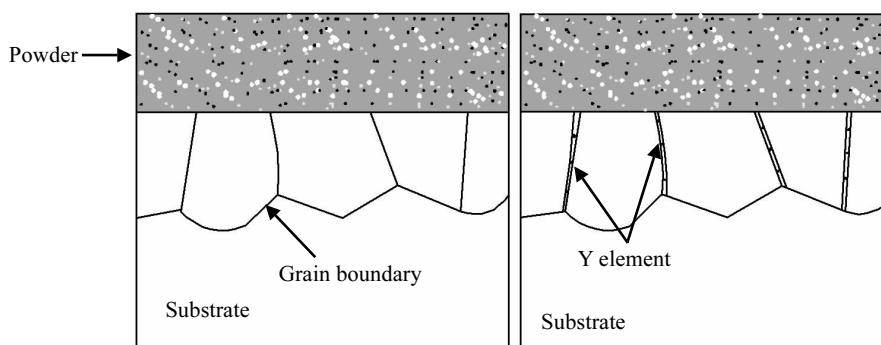


Fig. 8 Mechanism of rare earth promoting the formation of aluminum coatings

oxidation film to prevent oxygen from diffusion into the alloys at the early stage of the oxidation at 1000 °C. Subsequently the oxides (NiO) react with Cr_2O_3 to produce spinel NiCr_2O_4 ^[23,24], which is a disadvantage of the oxidation film. Meanwhile, TiO_2 grows up gradually on the top layer, which makes the oxidation film loose, due to the higher diffusion rate of Ti^{4+} compared to that of Cr^{3+} ^[25]. Finally, some oxidation scales are spalled under the condition of thermal stress.

Since the Al content in the outer layer of the coatings is very high, the selective oxidation will be generated to quickly form an Al_2O_3 oxidation film on the surface. The continuous and dense Al_2O_3 layer can work as a barrier to restrain oxygen diffusion into the substrate^[26]. The Cr-Co-Y-modified aluminide coating shows more excellent resistance to high temperature oxidation than the substrate. It is owing to a continuous and dense oxidation film composed of $\alpha\text{-Al}_2\text{O}_3$ ^[27] which is more stable than Cr_2O_3 at 1000 °C for a long time. As the oxidation proceeds, the Al element is consumed gradually. When the content of Al in the coating drops to the critical

point, elements like Cr, Ti, Co, Ni in the coating could be oxidized^[28]. These oxides are less protectable to the substrate compared with alumina.

The SEM image and EDS elemental mapping for Cr-Co- Y_2O_3 modified aluminide coating after oxidation at 1000 °C for 100 h are shown in Fig.9 and Fig.10, respectively. The layer of

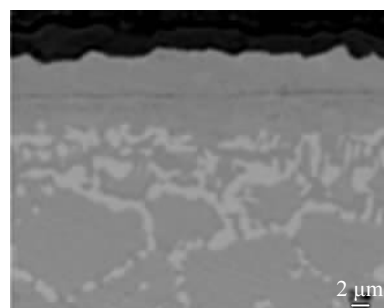


Fig. 9 SEM image of Cr-Co-Y-modified aluminide coating after oxidation at 1000 °C for 100 h

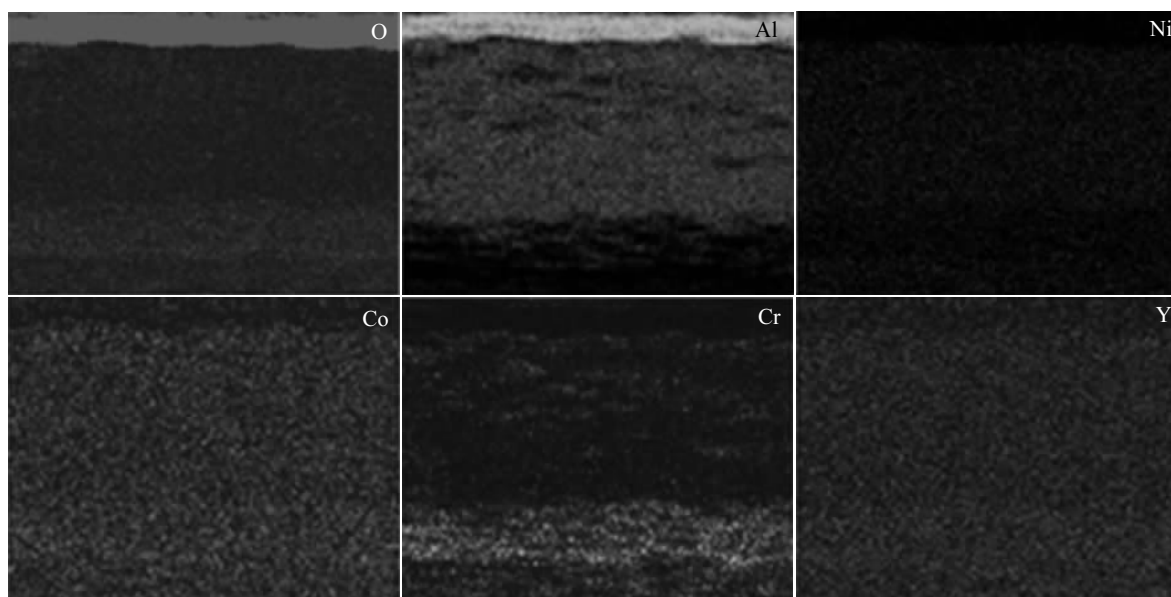


Fig. 10 EDS element mapping of O, Al, Ni, Co, Cr, Y for Cr-Co-Y-modified aluminide coating after oxidation at 1000 °C for 100 h

oxidation product is rich in Al and O, indicating that Al_2O_3 is formed at outer layer. Some of Cr is present in the inner layer and diffusion layer, which restrain the outward diffusion of Ni and other elements of the substrate. It can be concluded that the interdiffusion between the coating and the substrate occurs. The Cr(W) rich phases in the coating may cause two opposite processes at the high temperature: growth and dissolution^[29,30]. In the initial stages of oxidation, the growth is predominating. The Cr(W) rich phases grow up by almost swallowing Cr and refractory elements, and act as a diffusion barrier to restrain the interdiffusion between the coating and the substrate^[30,31]. With the extension of oxidation time, plenty of the Cr(W) rich phases are gathered in the grain boundaries, and others are dissolved in the γ/γ' phases due to its high solubility^[22], which leads to an aggravation in thermal diffusion.

3 Conclusions

1) The Cr-Co- Y_2O_3 modified aluminide coatings on the superalloy GH586 are achieved by pack process method with different contents of Co, Cr and Al. The thickness and high oxidation rate at 1000 °C for 100 h can be set as these coatings quality criteria.

2) The Cr-Co- Y_2O_3 modified aluminide coating has a mass gain of only 0.36 mg/cm² after oxidation at 1000 °C for 100 h. The parabolic rate constant of the coating is two orders of magnitude smaller than that of the substrate at 1000 °C. The coating exhibits a more excellent resistance to high temperature oxidation compared to the substrate.

3) The thermal diffusion of the coating is greatly influenced by Cr(W) phases after oxidation at 1000 °C for 100 h. At the beginning of oxidation, the Cr(W) rich phases grow up, which can act as a diffusion barrier to restrain the interdiffusion between the coating and the substrate. As the oxidation proceeds, a part of the Cr(W) rich phases are gathered in the grain boundaries, and others are gradually dissolved in the γ/γ' phases due to its high solubility, which may accelerate degradation of the coating.

References

- 1 Fritscher K, Leyens C, Schulz U. *Materials Science & Engineering A*[J], 2004, 369(1): 144
- 2 Das D K. *Progress in Materials Science*[J], 2013, 58(2): 151
- 3 Jiang S M, Li H Q, Ma J et al. *Corrosion Science*[J], 2010, 52(7): 2316
- 4 Zhang K, Wang Q M, Sun C et al. *Corrosion Science*[J], 2008, 50(6): 1707
- 5 Jackson R D, Taylor M P, Evans H E et al. *Oxidation of Metals*[J], 2011, 76(3-4): 259
- 6 Hesnawi A, Li H, Zhou Z et al. *Vacuum*[J], 2007, 81(8): 947
- 7 Lu J, Zhu S, Wang F. *Surface & Coatings Technology*[J], 2011, 205(21-22): 5053
- 8 Lu J, Zhu S, Wang F. *Oxidation of Metals*[J], 2011, 76(1-2): 67
- 9 Jamali H, Mozafarinia R, Razavi R S et al. *Ceramics International*[J], 2012, 38(8): 6705
- 10 Cui Q, Seo S M, Yoo Y S et al. *Surface & Coatings Technology*[J], 2015, 284: 69
- 11 Shi L, Xin L, Wei H et al. *Materials Science Forum*[J], 2015, 816: 289
- 12 Palcut M, Priputen P, Kusý M et al. *Corrosion Science*[J], 2013, 75(7): 461
- 13 Hounninou C, Chevalier S, Larpin J P. *Applied Surface Science*[J], 2004, 236(1-4): 256
- 14 Zhou C, Xu H, Gong S et al. *Surface & Coatings Technology*[J], 2000, 132(2-3): 117
- 15 Zhou W, Zhao Y G, Qin Q D et al. *Materials Science & Engineering A*[J], 2006, 430(1-2): 254
- 16 Ford S, Kartono R, Young D J. *Surface & Coatings Technology* [J], 2010, 204(12-13): 2051
- 17 Qiao M, Zhou C. *Corrosion Science*[J], 2012, 63(10): 239
- 18 Zhao X, Zhou C. *Corrosion Science*[J], 2014, 86(9): 223
- 19 Liu Z, Zhao X, Zhou C. *Corrosion Science*[J], 2015, 92: 148
- 20 Guo Jianting. *Materials Science and Engineering for Superalloys* [M]. Beijing: Science Press, 2008: 33 (in Chinese)
- 21 Pint B A, Haynes J A, Besmann T M. *Surface & Coatings Technology*[J], 2010, 204(20): 3287
- 22 Cao J, Zhang J, Hua Y et al. *Materials Characterization*[J], 2017, 125: 67
- 23 Cao Jiangdong, Zhang Junsong, Hua Yinqun et al. *Rare Metals*[J], 2017, 118(11): 1
- 24 Cao J, Zhang J, Hua Y et al. *Journal of Materials Processing Technology*[J], 2016, 243: 31
- 25 Cao J, Zhang J, Hua Y et al. *Surface & Coatings Technology*[J], 2017, 311: 19
- 26 Liu P S, Liang K M, Gu S R. *Corrosion Science*[J], 2001, 43(7): 1217
- 27 Pint B A. *Surface & Coatings Technology*[J], 2004, s188-189(1): 71
- 28 Zhang Y, Haynes J A, Wright G et al. *Metallurgical & Materials Transactions A*[J], 2001, 32(7): 1727
- 29 Fan Q X, Peng X, Yu H J et al. *Corrosion Science*[J], 2014, 84(8): 42
- 30 Zhang K, Wang Q M, Sun C et al. *Corrosion Science*[J], 2008, 50(6): 1707
- 31 Xu C Z, Jiang S M, Bao Z B et al. *Corrosion Science*[J], 2009, 51(6): 1467

粉末包埋法制备 Co-Cr-Y₂O₃ 改性铝化物涂层的高温氧化行为

曹将栋¹, 龚少军¹, 仲崇贵², 姚艳斌³

(1. 江苏航运职业技术学院, 江苏 南通 226010)

(2. 南通大学, 江苏 南通 226001)

(3. 深圳市注成科技股份有限公司, 广东 深圳 518001)

摘要: 为了提高高温合金的抗高温氧化性能, 采用粉末包埋法通过 Co-Cr-Y₂O₃ 改性铝化物涂层, 并对改性后的涂层进行微观组织结构 and 高温氧化行为的研究。结果表明: 经 X 射线衍射分析, 涂层主要的成分是 NiAl 相, 经 1000℃氧化 100 h, 其表面的氧化膜主要包含 Al₂O₃, Cr₂O₃ 和少量的 CoCr₂O₄。涂层的氧化动力学显示, 其平均氧化增重仅为 0.36 mg/cm², 明显低于基体氧化时的增重。结合涂层的表面和截面的氧化物的形貌, 可以看出涂层具有更好的抗高温氧化性能。同时在氧化过程中发现, 富 Cr(W)相在晶界聚集, 有利于 Cr 离子向表面的扩散而形成氧化膜, 并且阻碍了 Ti 离子向表面扩散的通道, 有助于抗高温氧化性能。

关键词: 高温合金; 高温氧化行为; 表面改性; 涂层

作者简介: 曹将栋, 男, 1979 年生, 博士, 副教授, 江苏航运职业技术学院机电系, 江苏 南通 226010, 电话: 0513-85960874, E-mail: caojd@ntsc.edu.cn